Endoplasmic Reticulum-Quality Control Chaperones Facilitate the Biogenesis of Cf Receptor-Like Proteins Involved in Pathogen Resistance of Tomato[1][C][W]

Thomas W.H. Liebrand, Patrick Smit, Ahmed Abd-El-Haliem[2], Ronnie de Jonge, Jan H.G. Cordewener, Antoine H.P. America, Jan Sklenar, Alexandra M.E. Jones, Silke Robatzek, Bart P.H.J. Thomma, Wladimir I.L. Tameling, and Matthieu H.A.J. Joosten*

Laboratory of Phytopathology, Wageningen University, 6708 PB Wageningen, The Netherlands (T.W.H.L., P.S., A.A.-E.-H., R.d.J., B.P.H.J.T., W.I.L.T., M.H.A.J.J.); Plant Research International, Wageningen University and Research Centre, 6708 PB Wageningen, The Netherlands (J.H.G.C., A.H.P.A.); Sainsbury Laboratory, Norwich Research Park, Norwich NR4 7UH, United Kingdom (J.S., A.M.E.J., S.R.); and Centre for BioSystems Genomics, 6700 AB Wageningen, The Netherlands (T.W.H.L., J.H.G.C., A.H.P.A., B.P.H.J.T., M.H.A.J.J.)

Cf proteins are receptor-like proteins (RLPs) that mediate resistance of tomato (*Solanum lycopersicum*) to the foliar pathogen *Cladosporium fulvum*. These transmembrane immune receptors, which carry extracellular leucine-rich repeats that are subjected to posttranslational glycosylation, perceive effectors of the pathogen and trigger a defense response that results in plant resistance. To identify proteins required for the functionality of these RLPs, we performed immunopurification of a functional Cf-4-enhanced green fluorescent protein fusion protein transiently expressed in *Nicotiana benthamiana*, followed by mass spectrometry. The endoplasmic reticulum (ER) heat shock protein70 binding proteins (BiPs) and lectin-type calreticulins (CRTs), which are chaperones involved in ER-quality control, were copurifying with Cf-4-enhanced green fluorescent protein. The tomato and *N. benthamiana* genomes encode four BiP homologs and silencing experiments revealed that these BiPs are important for overall plant viability. For the three tomato CRTs, virus-induced gene silencing targeting the plant-specific *CRT3a* gene resulted in a significantly compromised Cf-4-mediated defense response and loss of full resistance to *C. fulvum*. We show that upon knockdown of *CRT3a* the Cf-4 protein accumulated, but the pool of Cf-4 protein carrying complex-type *N*-linked glycans was largely reduced. Together, our study on proteins required for Cf function reveals an important role for the CRT ER chaperone CRT3a in the biogenesis and functionality of this type of RLP involved in plant defense.

Recognition of nonself molecules by immune receptors, of which a class is represented by resistance proteins, initiates plant immune responses, leading to resistance to invading pathogens (Chisholm et al., 2006; Jones and Dangl, 2006). In tomato (*Solanum lycopersicum*), the extracellular biotrophic fungal pathogen *Cladosporium fulvum* causes leaf mold disease and by the secretion of effector proteins its virulence is promoted (van den Burg et al., 2006; van Esse et al., 2007; Bolton et al., 2008; Stergiopoulos and de Wit, 2009; de Jonge et al., 2010). Recognition of *C. fulvum* race-specific effector proteins (also referred to as avirulence [Avr] proteins) by resistant tomato plants is mediated by Cf proteins. Cf proteins are transmembrane proteins that are classified as receptor-like proteins (RLPs), carrying an extracellular Leu-rich repeat (LRR) domain but lacking an obvious intracellular signaling domain, which is in contrast to receptor-like kinases (RLKs) that possess an intracellular kinase domain (Rivas and Thomas, 2005). Recognition of an effector of *C. fulvum* by the matching Cf protein triggers the activation of defense responses that eventually results in resistance to *C. fulvum*, a mechanism commonly referred to as effector-triggered immunity (Jones and Dangl, 2006). In this interaction, resistance is associated with the hypersensitive response (HR), which is a form of localized programmed cell death (de Jong et al., 2004; Rivas and Thomas, 2005; Jones and Dangl, 2006).

The biogenesis of functional transmembrane receptors, which involves proper folding and posttranslational modifications such as glycosylation, takes place in the

[1] This work was supported by the Graduate School Experimental Plant Sciences (to T.W.H.L.). T.W.H.L, J.H.G.C, A.H.P.A., B.P.H.J.T., and M.H.A.J.J. are subsidized by the Centre for BioSystems Genomics (part of the Netherlands Genomics Initiative and the Netherlands Organization for Scientific Research). P.S. and W.I.L.T. are supported by a VENI grant of the Netherlands Organization for Scientific Research (grant nos. 863.10.015 and 863.08.018, respectively). A.A.-E.-H. is supported by a Mosaic grant of the Netherlands Organization for Scientific Research (grant no. 017.003.046). J.S., A.M.E.J., and S.R. are supported by the Gatsby Charitable Foundation.

[2] Present address: Plant Breeding, Wageningen University, 6708 PB Wageningen, The Netherlands.

* Corresponding author; e-mail matthieu.joosten@wur.nl.

The author responsible for distribution of materials integral to the findings presented in this article in accordance with the policy described in the Instructions for Authors (www.plantphysiol.org) is: Matthieu H.A.J. Joosten (matthieu.joosten@wur.nl).

[C] Some figures in this article are displayed in color online but in black and white in the print edition.

[W] The online version of this article contains Web-only data.

www.plantphysiol.org/cgi/doi/10.1104/pp.112.196741

endoplasmic reticulum (ER). To prevent secretion of immature immune receptors not competent of ligand binding, to the plasma membrane a strict control mechanism of the different steps in protein maturation is required. ER-quality control (QC) is a process that involves several pathways, all ensuring that eventually only mature, correctly folded proteins are transported to their final cellular destination (Anelli and Sitia, 2008). One important pathway requires the abundant ER heat shock protein70 (HSP70) chaperones, referred to as binding proteins (BiPs). These BiPs form a complex with the HSP40-like cochaperones containing J domains (ERdj3) and stromal-derived factor-2 (Jin et al., 2008; Nekrasov et al., 2009; Schott et al., 2010). The BiP complex aids in client protein folding, thereby preventing protein aggregation, and is involved in ER-stress signaling (Anelli and Sitia, 2008). A second ER-QC pathway involves *N*-linked glycosylation and lectin chaperone-assisted folding of nascent proteins. *N*-linked glycosylation is initiated by addition of a $Glc_3Man_9GlcNAc_2$ oligosaccharide to Asn (N) residues of *N*-linked glycosylation sites with the consensus sequence (NxS/T), by the oligosaccharyltransferase complex. Glucosidase I and II cleave Glc residues from this glycan to leave monoglucosylated glycans on the client protein. Subsequently, the lectin chaperones calnexin (CNX) and calreticulin (CRT) are able to fold the client protein (Pattison and Amtmann, 2009). When correctly folded, glucosidase II removes the final Glc residue and the client protein is then translocated to the Golgi apparatus. Proteins that are still not correctly folded are reglucosylated by the folding sensor UDP-Glc glycoprotein glucosyltransferase and are subjected to another round of CNX/CRT-assisted folding. Glycoproteins that are still not properly folded are recognized by specific lectins with mannosidase activity, causing Man trimming. The loss of Man moieties reduces the affinity for CNX/CRT, which is a signal for ER-associated protein degradation (Anelli and Sitia, 2008; Nakatsukasa and Brodsky, 2008). Eventually, the last step in ER-QC involves the formation of disulfide bonds between free thiol groups present in the client protein, a modification that is mediated by protein disulfide isomerases (Anelli et al., 2003; Gruber et al., 2006).

After ER-QC-assisted folding and glycosylation, proteins are transferred to the Golgi apparatus where the *N*-linked glycans are further modified into complex-type *N*-linked glycans. In plants, in the Golgi a β(1,2)-Xyl and α(1,3)-Fuc residue are linked to the precursor core glycans of glycoproteins (Schoberer and Strasser, 2011). Eventually, functional RLPs are anticipated to carry complex-type *N*-linked glycans as numerous putative *N*-linked glycosylation sites are for example present in the LRR domains of different Cf proteins (Piedras et al., 2000). Although the complexity of the *N*-linked glycans remains to be elucidated, mutational analysis of the 22 putative *N*-linked glycosylation sites present in the Cf-9 protein revealed that most of these sites are indeed glycosylated and contribute to Cf-9 activity. Four glycosylation sites are even essential for Cf-9 function and removing all glycans by PNGaseF treatment caused a strong mobility shift, showing that Cf-9 is heavily glycosylated (Piedras et al., 2000; van der Hoorn et al., 2005). The observation that functional Cf proteins are abundantly glycosylated indicates that this type of RLP requires stringent ER-QC for their maturation to biologically active proteins.

A number of studies have addressed the identification of proteins that are required for Cf function. To date, all Cf-interacting proteins were found by yeast (*Saccharomyces cerevisiae*)-two hybrid analyses, using the C terminus of Cf-9 as a bait (Laurent et al., 2000; Nekrasov et al., 2006). Attempts to isolate and characterize Cf complexes in vivo following a biochemical approach, have failed up till now. To identify factors interacting with Cf proteins, we C-terminally tagged Cf proteins with enhanced GFP (eGFP). By transient *Agrobacterium tumefaciens*-mediated expression in *Nicotiana benthamiana*, a Solanaceous plant in which Cf proteins are functional (Van der Hoorn et al., 2000), we produced the tagged Cf proteins, allowing immunopurification of Cf-eGFP-containing protein complexes using GFP affinity beads. We found BiP and CRT ER chaperones as copurifying proteins, pointing to an important role of ER-QC in the biogenesis of functional Cf proteins. We discovered that, when compared with Arabidopsis (*Arabidopsis thaliana*), tomato and *N. benthamiana* contain one additional *BiP* gene. Furthermore, the latter two plants carry two *CRT3-like* genes, instead of only one for Arabidopsis. Silencing of *CRT3a* resulted in severely compromised Cf-4 functionality in *N. benthamiana* and tomato and we found a strong reduction in complex-type *N*-linked glycosylation of the Cf protein is responsible for this phenotype. Altogether, we show in vivo interaction between Cf proteins and ER-QC chaperones upon transient expression of the Cf proteins in *N. benthamiana* and reveal an important role for CRT3a in the biogenesis of a tomato RLP that is involved in resistance to a fungal pathogen.

RESULTS

Cf-eGFP Fusion Proteins Are Functional and Cf-4-eGFP Is Efficiently Immunopurified from Transiently Transformed *N. benthamiana* Leaves

We chose eGFP to C-terminally tag various Cf proteins for which the matching effector from *C. fulvum* has been identified (Fig. 1A). We also eGFP tagged the Cf-like protein Peru2, which is a Cf homolog from *Solanum peruvianum* that shows constitutive activity when expressed in *N. benthamiana* and tobacco (*Nicotiana tabacum*; Wulff et al., 2004). *A. tumefaciens*-mediated transient transformation of the Cf-eGFP proteins, in combination with the matching or a nonmatching Avr effector of *C. fulvum* in tobacco, revealed functionality of the tagged Cfs as an HR occurred when a matching Cf-eGFP/Avr

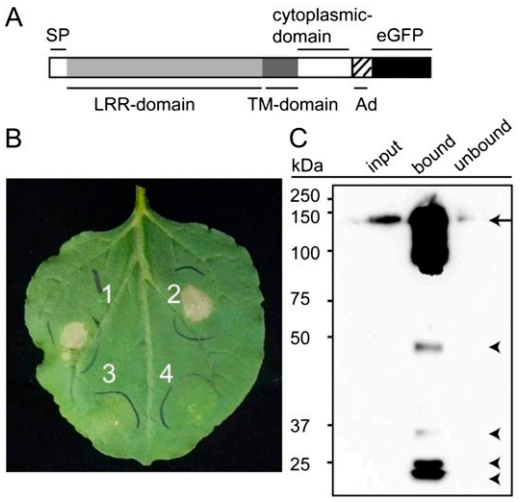

Figure 1. Tomato Cf proteins with a C-terminal eGFP tag are functional and are efficiently immunopurified using GFP affinity beads. A, Schematic representation of recombinant Cf proteins C-terminally tagged with eGFP. SP, Signal peptide; TM, transmembrane; Ad, cloning adapter. B, Coexpression of Cf-4-eGFP with the *C. fulvum* Avr4 effector by *Agrobacterium*-mediated expression in *N. benthamiana* results in a Cf-4/Avr4-specific HR (1). This HR developed equally fast and had the same intensity as the HR obtained upon coexpression of untagged Cf-4 with Avr4 (2). Cf-4-eGFP and untagged Cf-4 did not trigger an HR when coexpressed with the *C. fulvum* effector Avr9 (3 and 4, respectively). Leaves were photographed 3 d after *Agrobacterium* infiltration. C, Immunopurification of Cf-4-eGFP, transiently expressed in combination with the viral silencing suppressor P19 in *N. benthamiana*. A total protein extract of the infiltrated leaf tissue was subjected to immunopurification using GFP affinity beads. Total proteins (input), immunopurified proteins bound to the beads and eluted by boiling the beads in SDS sample buffer (bound), and proteins remaining in the supernatant (unbound) were separated by 8% SDS-PAGE and subjected to immunoblot analysis using αGFP antibody. The strong band at 140 kD has the size of Cf-4-eGFP (arrow). Putative Cf-4-eGFP degradation products are observed at 45, 37, and 20 kD. A band of 25 kD is observed at the expected size of free eGFP (arrowheads). [See online article for color version of this figure.]

pair was expressed (Supplemental Fig. S1). An HR was not observed when nonmatching Cf/Avr pairs were expressed, whereas the Peru2-eGFP fusion caused a constitutive HR (Supplemental Fig. S1). We also expressed Cf-4-eGFP in combination with Avr4 in *N. benthamiana* and similar results were obtained (Fig. 1B). The time period over which the HR developed and its intensity were similar to the HR caused by nontagged Cf-4.

We subsequently investigated whether we could immunopurify Cf-eGFP fusion proteins. Therefore, we transiently coexpressed Cf-4-eGFP with the P19 silencing suppressor in *N. benthamiana* and incubated a total protein extract of the infiltrated leaves with GFP affinity beads. Immunoblot analysis using an αGFP antibody revealed a specific band at about 140 kD (the M_r of Cf-4-eGFP) in the total protein extract (Fig. 1C, input) and a very strong signal in the eluate of the beads (Fig. 1C, bound), indicating successful immunopurification of the Cf-4 fusion protein.

The ER-Resident BiP and CRT Chaperones Copurify with Cf-4-eGFP

To identify Cf-4-eGFP copurifying proteins, *N. benthamiana* was transiently transformed with Cf-4-eGFP and the fusion protein was subjected to immunopurification with GFP affinity beads. Immunopurified proteins were separated by a short SDS-PAGE run and Coomassie stained. Two abundant proteins, one of approximately 140 kD and one of approximately 70 kD, were detected (Fig. 2A) and the bands were excised, subjected to in gel tryptic digestion, and the generated peptides were analyzed by mass spectrometry. The identification of peptide sequences originating from Cf-4-eGFP in the 140-kD band confirmed immunopurification of the Cf protein (Fig. 2B), whereas analysis of the 70-kD protein revealed several peptides originating from ER luminal BiPs, which are highly conserved members of the HSP70 family of chaperones. We identified several peptides originating from different Nb-BiP isoforms and projected them on the Sl-BiP1 sequence (Fig. 2C; Supplemental Table S1).

Following an alternative approach, we performed direct on-bead tryptic digestion upon immunopurification of Cf-4-eGFP, revealing that, besides BiPs, the ER lectin-like CRT chaperones copurified with the Cf-4 protein. Using a database consisting of Solanaceous plant protein sequences, we identified various peptides matching CRT proteins. We projected the identified peptides on the full-length tomato CRT protein sequences and found that a total of six unique peptides matched to the sequence of a tomato homolog of the plant-specific CRT3 class, which we named Sl-CRT3a (Fig. 2D; Supplemental Table S1). Furthermore, we found one peptide matching another tomato CRT3 homolog, here referred to as Sl-CRT3b (Fig. 2E; Supplemental Table S1), and three unique peptides matching a tomato CRT2 homolog, Sl-CRT2 (Fig. 2F; Supplemental Table S1). When we performed the same protocol on leaf tissue of *N. benthamiana* transiently expressing GUS in the presence of the P19 silencing suppressor, peptides matching to the BiP and CRT chaperones were not identified.

BiPs Interact with All Cfs Transiently Expressed in *N. benthamiana*

We studied the tomato *BiP* gene family using the tomato genome sequence (www.solgenomics.net) and identified four genes encoding BiP homologs (one more than in Arabidopsis; Noh et al., 2003), all containing a typical C-terminal HDEL-type ER-retention signal (Supplemental Fig. S2). We also investigated the *N. benthamiana BiP* family using existing databases to which recently the first draft of the *N. benthamiana* genome sequence was added (www.solgenomics.net), in

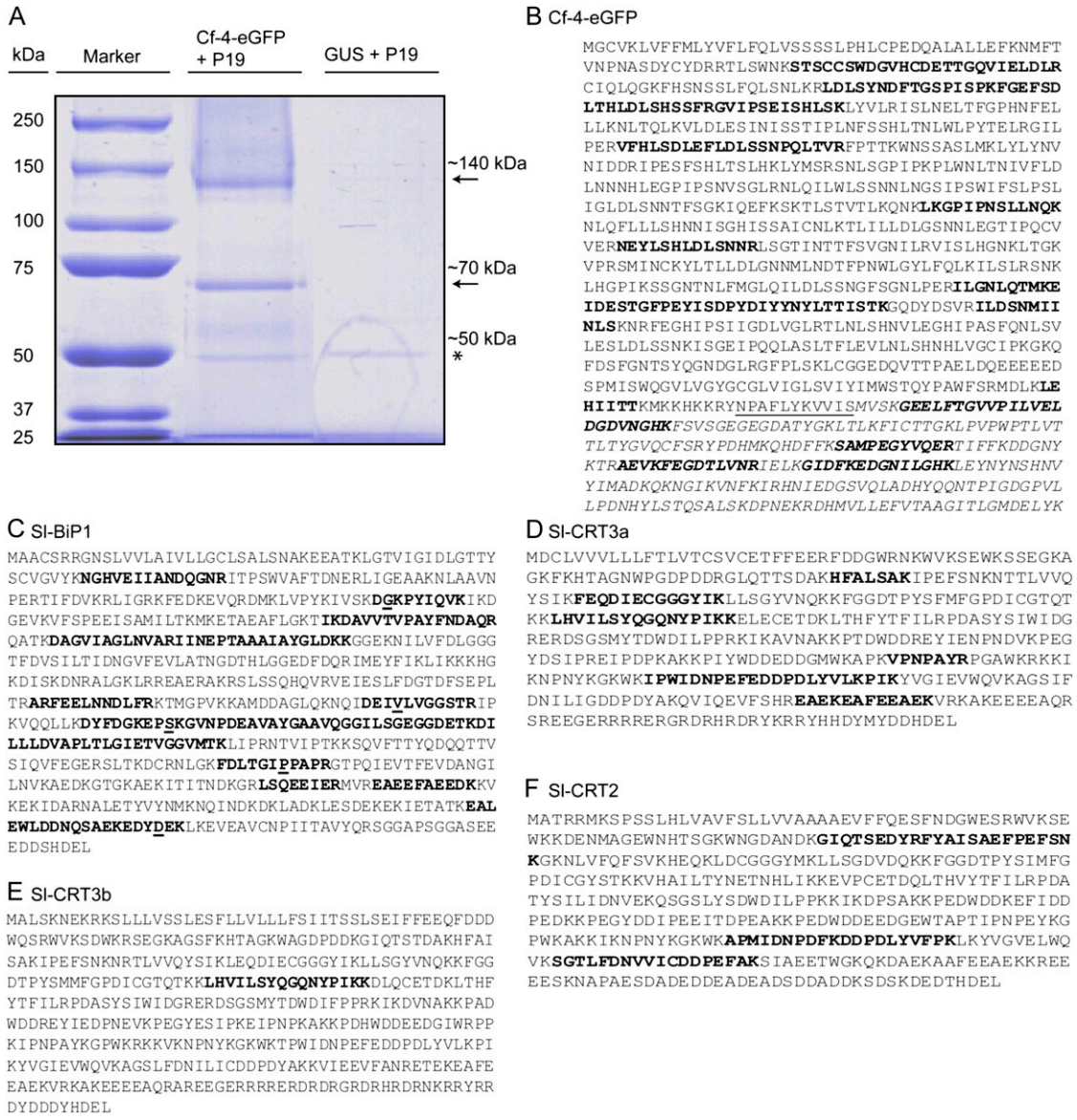

Figure 2. Immunopurification of Cf-4-eGFP reveals ER chaperones as copurifying proteins. A, Immunopurification with GFP affinity beads from *N. benthamiana* leaves transiently expressing Cf-4-eGFP or GUS. After pull down, beads were boiled in SDS sample buffer and the eluted proteins were separated by SDS-PAGE and Coomassie stained. Protein bands specific for the Cf-4-eGFP pull down were present at 140 and 70 kD (arrows), whereas a 50-kD protein band also copurified in the GUS control (asterisk). B, Coverage map of identified Cf-4-eGFP peptides originating from the protein band migrating at 140 kD, shown in section A. The Cf-4-eGFP protein sequence is shown and underlined is the cloning adaptor sequence that has been inserted between Cf-4 and eGFP. The eGFP sequence is depicted in italics and in bold the identified Cf-4 and eGFP peptides are shown. C, Coverage map of identified Nb-BiP peptide sequences originating from the 70-kD protein as shown in section A, projected on the Sl-BiP1 protein sequence. Sequences of the identified peptides are depicted in bold. Individual amino acids both depicted in bold and underlined indicate the position where the Nb-BiP sequence differs from the Sl-BiP1 sequence. D to F, Coverage maps of Nb-CRT peptide sequences (depicted in bold) identified upon analysis of total tryptic on-bead digests and projected on the corresponding Sl-CRT3a (D), Sl-CRT3b (E), and Sl-CRT2 (F) protein sequences. [See online article for color version of this figure.]

addition to RNA sequencing data from this plant (de Jonge et al., 2012). This also resulted in the identification of four distinct Nb-*BiP* genes. However, two Nb-*BiP* genes, Nb-*BiP2* and Nb-*BiP4*, are highly homologous to each other (Supplemental Fig. S2). A phylogenetic tree based on the Arabidopsis, tomato, and *N. benthamiana* BiP protein sequences is presented in Supplemental Figure S3A.

To determine whether BiPs only interact with Cf-4 or also with other Cf proteins, we transiently expressed eGFP-tagged Cf-2.2, Cf-4, Cf-4E, Cf-9, and the autoactive Cf-homolog Peru2 all C-terminally

fused to eGFP. We were able to express and purify all fusion proteins. However, using αGFP antibody, when expressed in the absence of P19 we detected a much weaker Cf-4-eGFP signal (Fig. 3, A and B) and only after a longer exposure a Cf-4-eGFP signal was revealed (Fig. 3C). Duplicate blots were incubated with an αBiP antibody, revealing that BiPs copurified with all Cf proteins, as well as with the autoactive Cf-homolog Peru2 (Fig. 3D). Upon overexposure of the immunoblot, we also detected a BiP signal for Cf-4-eGFP expressed in the absence of P19. So, even at low expression levels we found interaction of the BiPs with Cf-4-eGFP (Fig. 3E). As expected, BiPs did not copurify with the cytosolic GFP-hemagglutinin (HA) control fusion protein, a protein that does not pass the ER (Fig. 3, F and G). Together, these results show that BiPs interact with various Cf proteins and that the BiP ER-QC pathway is used by all of these RLPs.

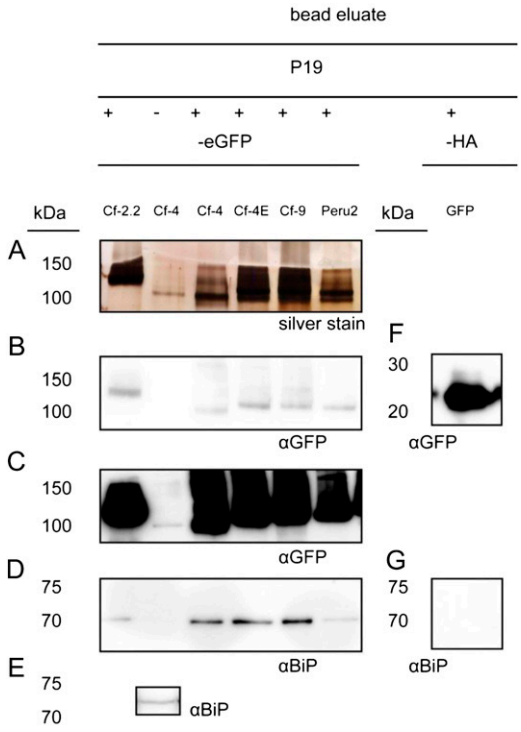

Figure 3. BiP interacts with various Cf proteins. The eGFP-tagged Cf proteins and autoactive Cf-like protein Peru2 and GFP-HA were expressed with P19 (+). Cf-4 was also expressed without P19 (−). Total protein extracts were subjected to immunopurification and proteins present in the eluate of the GFP affinity beads (bead eluate) were separated by 8% SDS-PAGE and silver stained (A) or analyzed by immunoblotting (B–G). A, Silver-stained immunopurified Cf proteins and Peru2. B, Proteins shown in A, analyzed by immunoblotting using αGFP antibodies, with 1 min of exposure time. C, Proteins shown in A, analyzed by immunoblotting using αGFP antibodies, with 5 min of exposure time. Note that Cf-4-eGFP is now also detected when not coexpressed with P19. D, A duplicate blot as shown in B and C was incubated with αBiP to reveal BiP as a copurifying protein. E, Overexposure of the blot shown in D. Note that BiP also copurifies with Cf-4 when expressed in the absence of P19. F, Immunopurified GFP-HA, as detected by αGFP antibodies. G, A duplicate blot as in F, now incubated with αBiP as primary antibody. Note that BiP does not copurify with GFP-HA. Representative results from three independent experiments are shown. [See online article for color version of this figure.]

Silencing of Multiple *BiPs* Causes Lethality in *N. benthamiana*

To investigate the role of the BiP chaperones in Cf-4 biogenesis, we generated tobacco rattle virus (TRV)-based virus-induced gene silencing (VIGS) constructs to knockdown the encoding genes in *N. benthamiana* expressing *Cf-4*. These plants were then transiently transformed to express Avr4 to test whether their responsiveness to this matching effector is compromised. As the tomato genome sequence was already available much earlier than the *N. benthamiana* genome sequence, we used the sequence information of the tomato *BiP* family to generate TRV inserts for VIGS of *BiP1*, *BiP2*, *BiP3*, or *BiP4* in *N. benthamiana*. In addition, we generated VIGS fragments simultaneously targeting three *BiPs* (TRV insert *BiP-1*, *-2*, and *-4*) and targeting all four *BiPs* (TRV insert *BiP-1*, *-2*, *-3*, and *-4*; see Supplemental Fig. S2; Supplemental Materials and Methods S1). Upon examining the *N. benthamiana* genome sequence in combination with the RNA sequencing data (de Jonge et al., 2012), we observed that the fragments *BiP1*, *BiP3*, *BiP-1*, *-2*, and *-4* and *BiP-1*, *-2*, *-3*, and *-4* target the corresponding *N. benthamiana* homologs. However, due to the high overall homology between Nb-*BiP2* and Nb-*BiP4*, the generated VIGS fragments targeting *BiP2* or *BiP4*, in fact target both genes simultaneously.

It has been reported previously that RNA interference-mediated gene silencing of all three *BiP* homologs in Arabidopsis is lethal (Hong et al., 2008). Therefore we first monitored the *N. benthamiana* plants for aberrant phenotypes over a period of 3 weeks after inoculation with the different recombinant TRV silencing constructs. VIGS of single *BiPs* did not result in aberrant phenotypes (Supplemental Fig. S4A). Similarly, we did not observe an aberrant phenotype upon inoculation with TRV:Sl-*BiP2* or TRV:Sl-*BiP4*, which are both targeting *BiP2* and *BiP4* simultaneously (Supplemental Fig. S4A). However, about 10 d after inoculation with the TRV construct targeting all four *BiPs* lethality was observed (Supplemental Fig. S4A). A similar, albeit weaker, phenotype was observed when three *BiPs* (*BiP1*, *BiP2*, and *BiP4*) were targeted (Supplemental Fig. S4A). These observations suggest that BiPs act redundantly and that in *N. benthamiana* silencing of multiple *BiPs* severely compromises viability.

To determine whether particular BiPs are specifically required for the biogenesis of Cf-4 proteins, we inoculated *N. benthamiana* expressing *Cf-4* with the different VIGS constructs targeting the individual *BiPs*. TRV:*Cf-4* was included as positive control, whereas TRV:*GUS* served as a negative control. Three weeks after TRV inoculation, fully expanded leaves were transiently transformed to express Avr4 to test the

plants for Cf-4 functionality (Van der Hoorn et al., 2000). To check whether the plants were still able to mount an HR, an autoactive variant of the NB-LRR immune receptor Rx (RxD460V; Bendahmane et al., 2002) and the proapoptotic factor Bcl2-Associated Protein X (BAX; Lacomme and Santa Cruz, 1999) were expressed in the same leaf. Inoculation with the different VIGS constructs targeting the individual *BiPs* did not compromise the Avr4-triggered HR, indicating full Cf-4 functionality. RxD460V- and BAX-triggered cell death also still occurred in these plants (Supplemental Fig. S4B). By contrast, when *Cf-4* itself was targeted a compromised Avr4-triggered HR was observed, whereas the response to RxD460V and BAX was not affected (Supplemental Fig. S4B).

Cf-4 Copurifies with the Different Tomato CRT Homologs When Transiently Coexpressed in *N. benthamiana*

We identified three genes encoding CRT homologs, all carrying an HDEL ER retention motif, in the tomato genome sequence (Supplemental Fig. S5). In Arabidopsis also three *CRTs* are present. Interestingly, this species has one *CRT* homolog that is specific for plants (At-*CRT3*; Persson et al., 2003; Jia et al., 2009; Jin et al., 2009), whereas tomato has two *CRTs* that are highly homologous to At-*CRT3*. We named these *CRTs* Sl-*CRT3a* and Sl-*CRT3b*. The third tomato *CRT*, Sl-*CRT2*, is most homologous to At-*CRT1* and At-*CRT2*. We also investigated the *N. benthamiana CRT* family and could clearly distinguish three Nb-*CRT* homologs. Like tomato, *N. benthamiana* has three *CRT* homologs of which two are most homologous to At-*CRT3* (Supplemental Fig. S5). However, given the fact that we observed single-nucleotide polymorphisms in the *N. benthamiana CRTs*, it is very likely that *N. benthamiana* has duplicates of several *CRT* homologs, due to the amphidiploid nature of this plant species. A phylogenetic tree based on the Arabidopsis, tomato, and *N. benthamiana* CRT protein sequences is presented in Supplemental Figure S3B.

We generated eGFP-tagged forms of the tomato CRTs (Sl-CRT2-eGFP, Sl-CRT3a-eGFP, and Sl-CRT3b-eGFP) and performed coimmunopurifications with Cf-4-Myc to determine whether the different tomato CRTs interact with this RLP. Confocal laser-scanning microscopy revealed that the C-terminal eGFP tag did not affect the subcellular localization of the CRTs, as all CRT-eGFP fusion proteins localized to the ER network upon transient expression in *N. benthamiana* (Supplemental Fig. S6). Coexpression of the CRT-eGFP fusions with Cf-4-Myc in *N. benthamiana*, followed by immunopurification of the CRTs with GFP affinity beads, revealed that Cf-4-Myc copurifies with all three Sl-CRTs (Fig. 4, A and C). The amount of copurified Cf-4-Myc correlated with the amounts of the different CRTs that were immunopurified, indicating that Cf-4 interacts with all Sl-CRTs to a similar extent. Cf-4-Myc did not copurify with the cytosolic GFP-HA protein (Fig. 4, B and D).

Nb-CRT3a Is Required for Functionality of the Cf-4 Protein in *N. benthamiana*

We next studied the role of the CRTs in Cf-4 function in *N. benthamiana*:*Cf-4* by VIGS. We generated specific *CRT2*, *CRT3a*, and *CRT3b* VIGS constructs based on the sequences of the *CRT* families of tomato and *N. benthamiana*, to establish individual *CRT* gene knockdowns. Upon comparison of the *CRT* sequences of tomato and *N. benthamiana*, we found that for

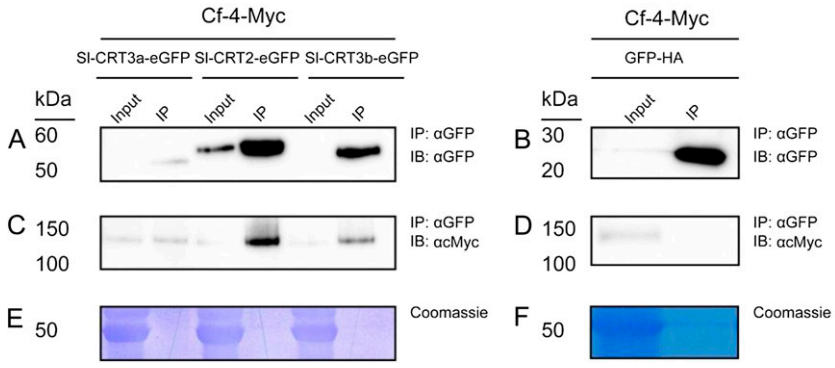

Figure 4. Cf-4 copurifies with the different tomato CRT homologs. Cf-4-Myc was expressed in combination with Sl-CRT3a-eGFP, Sl-CRT2-eGFP, Sl-CRT3b-eGFP, or GFP-HA in *N. benthamiana*. Total protein extracts of the transiently transformed leaf tissue were subjected to immunopurification using GFP affinity beads. Total proteins (Input) and immunopurified proteins (IP) were separated by SDS-PAGE and analyzed by immunoblotting. A and B, Immunoblots incubated with αGFP antibody, for detection of the immunopurified CRTs (A) or GFP-HA (B). Note that Sl-CRT3a-eGFP is accumulating to much lower amounts of protein than the other Sl-CRTs. C and D, Immunoblots incubated with αMyc antibody, for detecting copurified Cf-4-Myc. E and F, Coomassie-stained blots showing the 50-kD Rubisco band present in the total protein extract used as input for the immunopurifications shown in A to D, confirming equal loading. Representative results from three independent experiments are shown. [See online article for color version of this figure.]

targeting Nb-*CRT2* and Nb-*CRT3b*, a VIGS fragment based on the respective orthologous tomato *CRT* sequences can be used (TRV:Sl-*CRT2* and TRV:Sl-*CRT3b*), whereas for targeting Nb-*CRT3a* a silencing construct based on the *N. benthamiana CRT3a* sequence was required (TRV:Nb-*CRT3a*; Supplemental Fig. S5). Quantitative reverse transcription (qRT)-PCR analysis revealed that the three VIGS constructs knocked down the expression of the individual *CRTs* (Fig. 5A). We observed that in TRV:Sl-*CRT3b*-inoculated plants, in addition to Nb-*CRT3b* expression, Nb-*CRT3a* expression is reduced to some extent. This cross silencing is likely due to the high overall homology between both *CRT3* sequences (Supplemental Fig. S5). VIGS of the *CRTs* did not result in any aberrant morphological phenotype (Supplemental Fig. S7).

We tested whether silencing of the *CRTs* affects the Cf-4/Avr4-triggered HR. TRV:*Cf-4*, TRV:*GUS*, and TRV:*SGT1* inoculations were included as controls. Three weeks after inoculation of *N. benthamiana*:*Cf-4* plants with the various TRV constructs, leaves were transiently transformed to express Avr4, autoactive Rx (RxD460V), and the proapoptotic factor BAX. Interestingly, *CRT3a*-silenced plants showed a strongly reduced Avr4-triggered HR, whereas RxD460V- and BAX-triggered cell death remained unaltered in these plants when compared with the TRV:*GUS*-inoculated plants (Fig. 5B). In fact, the reduction in responsiveness to Avr4 of the *CRT3a*-silenced plants was similar to that of the TRV:*Cf-4*-inoculated plants. By contrast, *CRT2*- and *CRT3b*-silenced plants still mounted the Avr4-triggered HR (Fig. 5B). Silencing of *SGT1* resulted in loss of the response to all transiently expressed proteins (Fig. 5B). Together, these results indicate that Nb-*CRT3a* is essential for functionality of the Cf-4 protein in *N. benthamiana*.

Sl-*CRT3a* Is Required for Full Cf-4-Mediated Resistance of Tomato to *C. fulvum*

The compromised Cf-4-mediated HR due to knockdown of *CRT3a* expression in *N. benthamiana* prompted us to test whether *CRT3a* is also required for Cf-4-mediated resistance of tomato to an Avr4-producing strain of *C. fulvum*. *Cf-4*-expressing tomato plants were inoculated with the TRV:Sl-*CRT2* and TRV:Sl-*CRT3b* constructs and a TRV construct based on the tomato *CRT3a* sequence (TRV:Sl-*CRT3a*; Supplemental Fig. S5). Three weeks later the plants were inoculated with a strain of *C. fulvum* secreting Avr4 and transgenic for the *GUS* reporter gene. After another 2 weeks leaflets were stained for GUS activity to reveal fungal colonization of

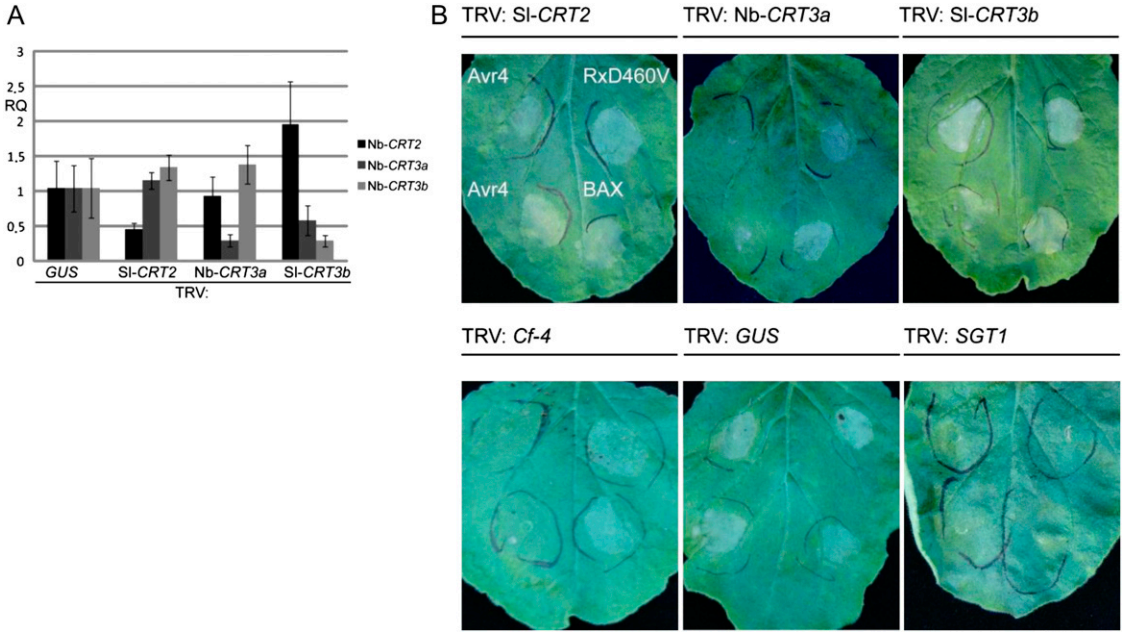

Figure 5. Nb-*CRT3a* is required for Cf-4 function in *N. benthamiana*. A, *N. benthamiana* was inoculated with the indicated TRV constructs and relative transcript levels (RQ) of Nb-*CRT2*, Nb-*CRT3a*, and Nb-*CRT3b* were determined by qRT-PCRs. The expression levels for each *CRT* gene were standardized to their expression levels in the TRV:*GUS*-inoculated plants. All samples were normalized to actin. The SD shows the variation between three technical repeats. B, Transgenic *N. benthamiana*:*Cf-4* plants were subjected to VIGS of the *CRTs* by inoculation with the TRV constructs indicated above each section. TRV:*Cf-4*, TRV:*GUS*, and TRV:*SGT1* served as controls. Three weeks after inoculation, Avr4 (in duplicate), autoactive Rx (RxD460V), and BAX were expressed by *Agrobacterium* infiltration in the order indicated in the first section. Leaves were photographed 3 d later. Note that similar to *Cf-4*-silenced plants, in the *CRT3a*-silenced plants the response to Avr4 is specifically suppressed. Representative results from three independent experiments are shown. In each independent experiment at least three plants were silenced per TRV construct. [See online article for color version of this figure.]

the leaf tissue. As controls, Cf-4 tomato plants inoculated with TRV:*Cf-4* and TRV:*GUS* were included. We also included fully susceptible Money Maker (MM)-Cf-0 tomato plants in each disease assay.

Strikingly, VIGS of *CRT3a* resulted in compromised Cf-4-mediated resistance to *C. fulvum* when compared with TRV:*GUS*-inoculated plants, as observed by the blue spots on the tomato leaflets, indicating fungal colonization of the leaf mesophyll (Fig. 6A). Resistance appeared to be compromised to a level more or less similar to that of Cf-4 tomato silenced for the *Cf-4* gene itself. Leaflets of TRV:Sl-*CRT2*- and TRV:Sl-*CRT3b*-inoculated plants did not show enhanced *C. fulvum* growth when compared with the TRV:*GUS* control (Fig. 6A). Quantitation of the amount of fungal colonization revealed that leaflets of TRV:Sl-*CRT3a*- and TRV:*Cf-4*-inoculated plants are significantly more intensely colonized by *C. fulvum*, than leaflets of the other plants (Fig. 6B).

Cf Proteins Contain Complex-Type *N*-Linked Glycans

Having established that knockdown of *CRT3a* gene expression compromises both Cf-4-mediated HR and resistance, we wanted to investigate the molecular basis of this observation. As CRTs are specifically involved in folding and maturation of glycoproteins, we reasoned that silencing of *CRT3a* results in compromised CRT3a-assisted folding, thereby affecting the transport of the Cf-4 protein to the Golgi, which is the cellular compartment where complex-type glycosylation

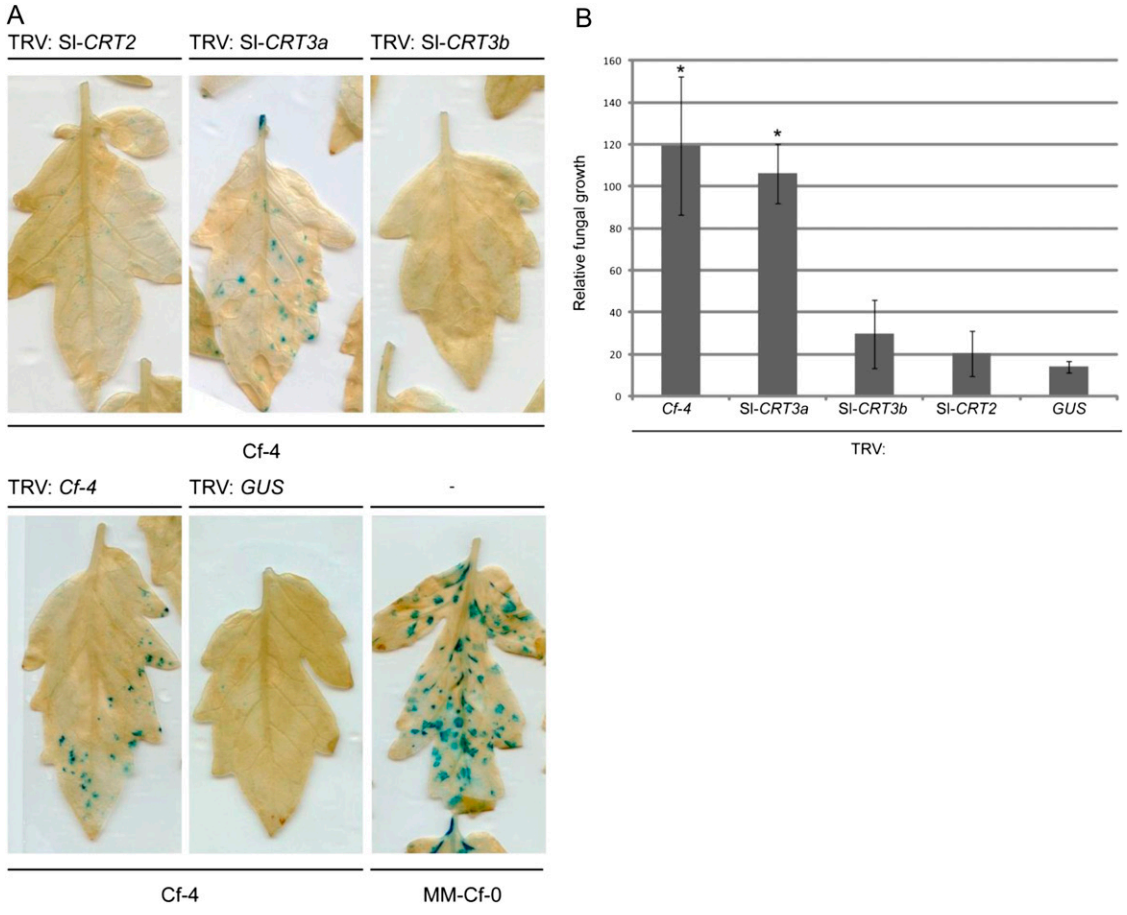

Figure 6. Sl-CRT3a is required for full Cf-4-mediated resistance of tomato to *C. fulvum*. A, Cf-4 tomato was inoculated with the indicated TRV constructs and noninoculated MM-Cf-0 was included as a *C. fulvum*-susceptible control. Three weeks after TRV inoculation of the Cf-4 plants, leaflets of all plants were inoculated with a strain of *C. fulvum* secreting *Avr4* and transgenic for the *GUS* gene. Two weeks later, leaflets were stained for GUS activity to detect fungal colonization, visible as blue-stained spots. B, Quantification of the colonization by *C. fulvum* of leaflets of Cf-4 tomato inoculated with the different TRV constructs by the ImageJ plug-in Phenotype Quant. The average relative fungal colonization in three independent experiments as shown in A was calculated and the error bars represent the SE of mean (SEM). For each experiment about 30 leaflets were scanned and examined for *C. fulvum* colonization by the quantification software. Asterisks indicate a statistically significant difference as compared with the TRV:*GUS*-inoculated plants (one-way ANOVA, $P < 0.05$). Three independent experiments were performed and representative results are shown. [See online article for color version of this figure.]

takes place. Hampered entry into the Golgi, then leads to a reduced pool of mature Cf protein containing complex-type *N*-linked glycans. First, we wanted to confirm that functional eGFP-tagged Cf proteins carry complex-type *N*-linked glycans. For this we made use of a polyclonal α horseradish peroxidase (αHRP) antibody directed against HRP, which is a heavily glycosylated protein containing many complex-type *N*-linked glycans that act as antigens. As a result, the αHRP antibody cross-reacts with proteins that are also subjected to this type of glycosylation (Henquet et al., 2008).

We immunopurified eGFP-tagged Cf-2.2, Cf-4, Cf-4E, Cf-9, and Peru2 from transiently transformed *N. benthamiana* leaves and after SDS-PAGE and blotting, one blot was incubated with αGFP antibody to detect the total amounts of immunopurified Cf proteins, whereas a duplicate blot was incubated with the αHRP antibody. Incubation with αGFP revealed that similar amounts of the Cf proteins were immunopurified (Fig. 7A). Incubation with αHRP antibody resulted in a clear signal at the expected size of the different Cf proteins, indicating that they all carry complex-type *N*-linked glycans (Fig. 7B). Interestingly, Cf-2.2 and Peru2 show a remarkably stronger signal than the other Cf proteins (Fig. 7B). On this blot, the detected complex glycosylated protein fraction most likely represents the pool of mature and biologically active transiently expressed Cf proteins.

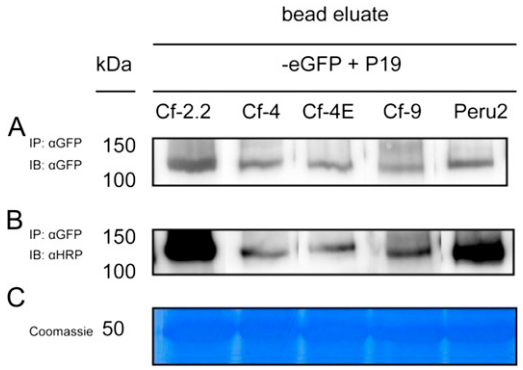

Figure 7. Transiently expressed Cf proteins contain complex-type *N*-linked glycans. Cf proteins and autoactive Peru2, all fused to eGFP, were transiently coexpressed with P19 in *N. benthamiana* and immunopurified using GFP affinity beads. The bead eluate was divided into two equal volumes and proteins were subjected to SDS-PAGE, followed by immunoblotting. A, Immunoblot incubated with αGFP antibody to reveal the amounts of purified eGFP-tagged Cf protein. B, A duplicate of the blot presented in A, but now incubated with αHRP to show the pool of complex glycosylated Cf protein. C, Coomassie-stained blot of the total protein extracts used as input for the immunopurifications showing the 50-kD Rubisco band to confirm equal loading. Representative results from three independent experiments are shown. For clarity, lanes from the same immunoblot and with the same exposure time were reordered. [See online article for color version of this figure.]

Nb-*CRT3a* Silencing in *N. benthamiana* Hampers Cf-4 Complex Glycosylation

To investigate whether Nb-*CRT3a* knockdown indeed reduces the pool of mature Cf protein containing complex-type *N*-linked glycans, we inoculated *N. benthamiana* with the different *CRT* VIGS constructs, including TRV:*GUS* as a control. We then expressed Cf-4-eGFP in silenced leaves, followed by Cf-4 immunopurification, SDS-PAGE, and immunoblotting. We determined the total amount of purified Cf-4 protein by incubation with αGFP antibody, whereas the relative amount of complex glycosylated Cf-4-eGFP protein was determined using αHRP antibody. The αGFP blot revealed that we purified similar amounts of Cf-4 protein from different *CRT*-silenced plants (Fig. 8A). Strikingly, VIGS of *CRT3a* almost completely abrogated the accumulation of Cf-4 carrying complex-type glycans (Fig. 8B). This phenomenon was also observed upon VIGS of *CRT3b*, albeit to a much lower extent (Fig. 8B). The pool of Cf-4 carrying complex-type glycans was not affected when *CRT2* was knocked down (Fig. 8B). Taken together, these results indicate that *CRT3a* is the most important lectin-like chaperone involved in Cf-4 protein folding, allowing subsequent transport of the protein to the Golgi apparatus for the generation of mature, complex glycosylated Cf-4 proteins.

DISCUSSION

ER-QC Chaperones Are Involved in Maturation of Transmembrane Immune Receptors

Here we show that the ER chaperones BiP and CRT are in planta interactors of Cf proteins (Figs. 2–4) and that CRT3a is the most important CRT lectin-type chaperone required for the biogenesis and maturation of complex glycosylated Cf proteins (Fig. 8). Several Arabidopsis mutants in the ER-QC pathway were recently identified to be immunocompromised in bacterial infections (Li et al., 2009; Nekrasov et al., 2009; Saijo et al., 2009). Mutants in the folding sensor UDP-Glc glycoprotein glucosyltransferase, the ERD2b HDEL receptor, and CRT3 were affected in the accumulation of the RLK EFR, which is the receptor for the bacterial pathogen-associated molecular pattern (PAMP) EF-Tu (elf18/26), and subsequent elf18-induced responses (Zipfel et al., 2006; Li et al., 2009; Nekrasov et al., 2009; Saijo et al., 2009; Christensen et al., 2010). Interestingly, *crt1* and *crt2* double mutants were hardly affected in elf18-induced responses, hence it was concluded that from the three Arabidopsis CRTs, CRT3 is the most important homolog for the biogenesis of functional EFR (Li et al., 2009; Saijo et al., 2009). Arabidopsis *crt3* knockout mutants were more susceptible to *Pseudomonas syringae* pv *tomato* DC3000 than *efr* mutants, suggesting that multiple immune receptors require CRT3-mediated ER-QC (Li et al., 2009). In line with this, we observed that silencing of a particular *CRT3* homolog in *N. benthamiana* and tomato, Sl-*CRT3a*,

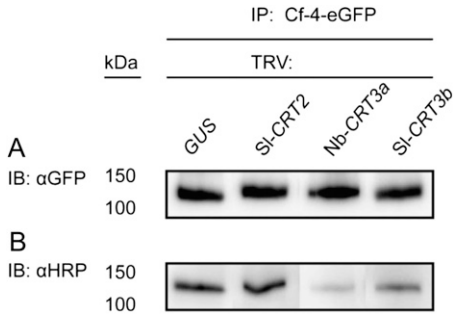

Figure 8. VIGS of *CRT3a* results in a reduction of the pool of Cf-4 protein carrying complex-type *N*-linked glycans. Cf-4-eGFP was transiently expressed in *N. benthamiana* leaves, silenced for the different *CRTs* as indicated above the sections. Two days after *Agrobacterium* infiltration, Cf-4-eGFP was immunopurified. The eluate from the beads was divided into two equal volumes and proteins were subjected to SDS-PAGE and immunoblotting. A, Immunoblot incubated with αGFP antibody to show the total amounts of immunopurified Cf-4-eGFP. B, A duplicate of the blot presented in A, but now incubated with αHRP antibody to reveal the pool of mature Cf-4 carrying complex-type glycans. Representative results from three independent experiments are shown. For clarity, lanes from the same immunoblot and with the same exposure time were reordered.

compromises Cf-4-mediated defense responses. This suggests that Cf-4 is a client of this CRT3 homolog.

Upon silencing of *CRT3a* in *N. benthamiana* we did not observe a reduced accumulation of the Cf-4 protein, despite compromised Cf-4-mediated responses and a nearly complete loss of the protein pool carrying complex-type *N*-linked glycans (Fig. 8). This suggests that due to lower CRT3a levels, Cf-4 cannot maturate in the Golgi apparatus and therefore does not undergo the full glycosylation required for its functionality. Immature PAMP receptors are prevented to reach the plasma membrane where they perceive their cognate PAMPs (Häweker et al., 2010). Hence, Cf-4 transport to the plasma membrane may also be affected when the amount of CRT3a lectin chaperone is limiting. Cf-4 functionality could also be lost because the underglycosylated Cf-4 protein cannot perceive the Avr4 ligand anymore or has become unstable upon exposure of the extracellular LRRs, which are normally highly glycosylated, to the apoplast.

The reason that we did not observe reduced Cf-4 protein accumulation upon *CRT3a* silencing could be due to the fact that VIGS does not completely knockout *CRT3a* expression (Fig. 5A). Interestingly, weakly defective *crt3* mutant plants accumulate EFR protein to normal levels, despite the hampered functionality of the PAMP receptor (Saijo et al., 2009). However, in these mutants elf26 ligand binding to EFR was greatly reduced. Hence, it was speculated that receptor abundance control and QC can be uncoupled and only the latter was hampered in weak *crt3* mutant plants. In that case our *CRT3a*-silenced *N. benthamiana* plants resemble the weak *crt3* Arabidopsis mutant. Lowered *CRT3b* expression levels also reduced the Cf-4 pool carrying complex-type *N*-linked glycans to some extent (Fig. 8). As CRT3a and CRT3b are highly homologous (Supplemental Figs. S3B and S5), VIGS of *CRT3b* also somewhat lowered the expression of *CRT3a* due to cross targeting by the *CRT3b* insert (Fig. 5A). Nevertheless, the mature pool of Cf-4 was sufficiently large and there was no effect on its function (Figs. 5, 6, and 8). We noticed an up-regulation of *CRT2* transcription in plants silenced for *CRT3b* (Fig. 5A). This upregulation might be required to compensate for the suppression of several cellular functions of the CRT3s. However, it is unlikely that higher *CRT2* expression levels affect the Cf-4/Avr4-mediated HR. As specific silencing of *CRT3a* strongly suppresses the Cf-4-mediatedHR (Fig. 5B) and in this plant *CRT2* expression levels (and also *CRT3b* expression levels) are very similar to the TRV:GUS-inoculated plants, the sufficiently high *CRT3a* expression levels in the *CRT3b*-silenced plant are the reason for an unaffected Cf-4/Avr4-mediated HR (Fig. 5A). In agreement with this, silencing of *CRT2* also does not lead to a reduced Cf-4-mediated HR.

Arabidopsis mutants in the BiP cochaperone stromal-derived factor-2 were also compromised in EFR signaling due to reduced accumulation of mature EFR protein (Nekrasov et al., 2009). In addition to affecting EFR levels, also the accumulation of the RLK FLAGELLIN SENSING2 (FLS2), responsible for recognition of the bacterial PAMP flagellin and its elicitor-active epitope flg22 (Gómez-Gómez and Boller, 2000), was affected to some extent (Nekrasov et al., 2009). In rice (*Oryza sativa*), Os-BiP3 was reported to interact with the RLK XA21, responsible for resistance to *Xanthomonas oryzae* pv *oryzae* (Park et al., 2010). Silencing of Os-*BiP3* did not lead to loss of XA21-mediated resistance in rice. However, overexpression of Os-*BiP3* resulted in reduced resistance to the bacterium due to induction of ER stress and enhanced XA21 proteolysis (Park et al., 2010). It remains to be elucidated whether overexpression of one or more Sl-BiPs will affect resistance of tomato to *C. fulvum*. Interestingly, two BiP chaperones were found to accumulate during the Cf-4/Avr4-triggered HR in tomato, suggesting that upregulation of BiPs is required for Cf-4-mediated resistance (Xu et al., 2012).

Recently, CRT2 and CRT3a of *N. benthamiana* were reported to be involved in effector-triggered immunity. Silencing of Nb-CRT2 and Nb-CRT3a reduced the accumulation of the membrane-localized, induced receptor kinase that is involved in immunity to *Tobacco mosaic virus* mediated by the NB-LRR-type immune receptor *N* (Caplan et al., 2009). This shows that the induced receptor kinase requires multiple CRTs for full functionality and accumulation. In addition to a role as a chaperone, Arabidopsis CRT2 was shown to regulate salicylic-acid-dependent expression of defense genes, with its C-terminal calcium-binding domain and amino acid residue H173 in its N-terminal chaperone domain playing an important role in this regulation (Qiu et al., 2012). We found that CRT3a is

specifically required for the maturation of Cf proteins to functional immune receptors. Together with the role of ER chaperones in EFR/FLS2-mediated PAMP responses and *N*-mediated resistance, we show that ER-QC is an essential layer of plant immunity, both in PAMP-triggered immunity as well as in effector-triggered immunity.

Regarding the HR assays in *N. benthamiana*:*Cf-4* inoculated with the various TRV constructs, care has to be taken with interpreting the results as Avr4 is expressed by *Agrobacterium* infiltration. The secreted Avr4 protein may also require ER chaperone-assisted folding and this process could also be affected upon VIGS of the different ER-QC chaperones. However, this is unlikely to be the case for the following reasons. Avr4 has only one putative *N*-linked glycosylation site that is not required for Avr4 function as an effector triggering Cf-4-mediated HR (van den Burg et al., 2001). Hence it is unlikely that Avr4 folding heavily depends on the CRTs. Furthermore, a clear decrease in the Cf-4 pool carrying complex *N*-linked glycans was observed upon *CRT3a* silencing in *N. benthamiana*, coinciding with compromised Avr4-triggered HR. Most importantly, in Cf-4-containing tomato, silencing of *CRT3a* leads to compromised resistance to a strain of *C. fulvum* that secretes Avr4 directly into the apoplast upon colonization of the leaflets. We can therefore exclude that hampered folding and/or translocation of Avr4 to the apoplast causes the suppressed HR in *CRT3a*-silenced *N. benthamiana*:*Cf-4*.

Proper Complex Glycosylation Is Required for Cf Protein Function

It was shown earlier that transiently expressed Cf-9 protein is heavily glycosylated on its extracellular LRRs. Furthermore, mutational analysis of the individual *N*-linked glycosylation sites in the LRR domain revealed that all sites, except one, are indeed glycosylated (Piedras et al., 2000; van der Hoorn et al., 2005). Glycosylation was found to be required for Cf-9 functionality, as introduction as well as removal of *N*-linked glycosylation sites reduced the Avr9-triggered HR (van der Hoorn et al., 2005). The complexity of the *N*-linked glycans was not determined in previous experiments. Here we show by using an αHRP antibody that binds to β(1,2)-Xyl and α(1,3)-Fuc residues (Henquet et al., 2008), that all Cf proteins contain complex-type glycans that are decorated with these residues.

Studies on EFR and FLS2 revealed that nearly all glycosylation sites of these receptors are also being occupied (Häweker et al., 2010; Sun et al., 2012). Mutations in STT3A, a member of the oligosaccharyltransferase complex, led to a loss of EFR-mediated immune responses and elf26 ligand binding, but did not affect FLS2-mediated responses (Nekrasov et al., 2009; Saijo et al., 2009; Häweker et al., 2010). Similar to the effects of specific mutations of glycosylation sites in Cf-9, *N*-linked glycosylation at specific residues was also found to be important for EFR function. For example, a single mutation at a conserved *N*-linked glycosylation site at position N143 results in an EFR mutant that is unable to bind elf26 and only accumulates to low levels (Häweker et al., 2010). Recently, two additional glycosylation sites (N342 and N366, respectively) were found to be crucial for EFR functionality (Sun et al., 2012). Strikingly, FLS2 functionality is much less dependent on ER-QC and *N*-linked glycosylation (Häweker et al., 2010; Sun et al., 2012). This was explained by proposing that EFR, in an evolutionary perspective, is relatively younger than FLS2. Such young immune receptors do not easily fold by themselves and are expected to require more stringent ER-QC for their biogenesis (Boller and Felix, 2009; Li et al., 2009; Saijo et al., 2009; Häweker et al., 2010).

Our data show that Cf proteins also rely heavily on ER-QC, suggesting that also these RLPs have only evolved recently. Indeed, *Cf* genes are arranged in large genomic clusters in which during meiosis crossovers occur that rapidly generate new Cf variants (Parniske et al., 1997; Parniske and Jones, 1999; Kruijt et al., 2004). When these new Cf proteins detect novel effectors they will be retained in the population. However, these new receptors have not yet been selected for proper intrinsic stability and therefore they heavily rely on ER-QC for their folding and functionality.

MATERIALS AND METHODS

Plant Material and Growth Conditions

Tobacco (*Nicotiana tabacum*), wild-type *Nicotiana benthamiana*, and transgenic *N. benthamiana*:*Cf-4* (Gabriëls et al., 2007) were grown in climate chambers under 16 h of light (150 μmol m^{-2} s^{-1}) at 25°C and 8 h of darkness at 21°C, at a relative humidity of approximately 75%. Tomato (*Solanum lycopersicum*), transgenic for the *Cf-4* resistance gene (Hcr9-4D; Thomas et al., 1997) was grown in the greenhouse under 16 h of light (100 W m^{-2} supplemental light when the intensity dropped below 150 W m^{-2}) at 21°C and 8 h of darkness at 19°C, at a relative humidity of approximately 75%.

Construction of Binary Vectors for *Agrobacterium*-Mediated Expression

The sequences of all oligonucleotide primers used in this study can be found in Supplemental Table S2. Full-length *Cf-2.2* was amplified by PCR on complementary DNA (cDNA) obtained from *Cf-2.2* expressing tomato using primers to13 and to14. *Cf-4* was amplified from plasmid pRH46 (Van der Hoorn et al., 2000) using primers to11 and to12 and *Peru2* was amplified from pWL111.5 (Wulff et al., 2004) using primers to22 and to23. PCR fragments of *Cf-2.2*, *Cf-4*, and *Peru2* were subsequently cloned into pDONR201 using Gateway BP clonase II (Invitrogen). *Cf-4E* was amplified with primers to129 and to130 from plasmid pRH471. *Cf-9* was obtained from pRH21 (Van der Hoorn et al., 2000) using primers to128 and to129. PCR fragments of *Cf-4E* and *Cf-9* were cloned into pENTR/D-Topo (Invitrogen). Sl-*CRT2*, Sl-*CRT3a*, and Sl-*CRT3b* were amplified from tomato cDNA using primer combinations to197 and to198, to195 and to196, and to199 and to200, respectively, and cloned into pENTR/D-Topo. All pDONR201 and pENTR/D-Topo constructs were sequenced to verify the sequence of the fragments and subsequently fragments were transferred to the binary vector pBIN-KS-35S::-GWY-eGFP (Sol 2095; for C-terminally tagging with eGFP) or pGWB20 (Nakagawa et al., 2007), using Gateway LR Clonase II, thereby generating pBIN-KS-35S::Cf-2.2-eGFP (Sol 2738), pBIN-KS-35S::Cf-4-eGFP (Sol 2701), pBIN-KS-35S::Cf-4E-eGFP (Sol 2737), pBIN-KS-35S::Cf-9-eGFP (Sol 2736), pBIN-KS-35S::Peru2-eGFP

(Sol 2739), pGWB20-Cf-4-Myc (Sol 2783), pBIN-KS-35S::Sl-CRT2-eGFP (Sol 2790), pBIN-KS-35S::Sl-CRT3a-eGFP (Sol 2789), and pBIN-KS-35S::Sl-CRT3b-eGFP (Sol 2791). Binary vectors used to express nontagged Cf-4 and Cf-9 were pRH48 and pRH21, respectively (Van der Hoorn et al., 2000). All binary vectors were transformed to *Agrobacterium tumefaciens* strain C58C1, carrying helper plasmid pCH32, for *Agrobacterium* infiltration assays. *Agrobacterium* infiltrations were performed as described previously (Van der Hoorn et al., 2000).

Immunopurifications of Transiently Expressed Tagged Proteins

Leaves of 6-week-old *N. benthamiana* plants were transiently transformed by *Agrobacterium*-mediated expression with pBIN-KS-35S::Cf-eGFP constructs (or the controls pBIN61-GUS or pBIN61-GFP-HA) and the P19 silencing suppressor (Voinnet et al., 2003) in a 1:1 ratio at a final OD_{600} = 1 for each construct. For the coimmunopurifications of Cf-4-Myc with the different Sl-CRTs-eGFP fusion proteins, constructs were infiltrated in a 1:1 ratio without P19 at an OD_{600} = 1 of each construct. For the immunopurification of Cf-4-eGFP from TRV-inoculated plants Cf-4-eGFP was infiltrated without P19 at an OD_{600} = 1. Two days after *Agrobacterium* infiltration, leaves were frozen in liquid nitrogen and ground to a fine powder using mortar and pestle. Proteins were extracted using radioimmunoprecipitation assay extraction buffer (150 mM NaCl, 1.0% IGEPAL CA-630 [NP-40], 0.5% sodium deoxycholate, 0.1% SDS, 50 mM Tris, pH 8.0), plus one complete protease inhibitor tablet (Roche) per 50 mL extraction buffer (1 g of leaf tissue [fresh weight] per 2 mL of extraction buffer was used). Samples were centrifuged at 4°C for 15 min at 18,000*g* and the supernatant was transferred to a new tube. For mass spectrometry analysis of proteins copurifying with the Cf proteins, 10 mL of total protein extract was incubated at 4°C for 3 h with 60 μL (50% slurry) of GFP-trap_A beads (Chromotek). For other immunopurifications, 2 mL of total protein extract was incubated at 4°C for 1 h with 15 μL (50% slurry) of the GFP-trap_A beads. After incubation, beads were collected by 1,000*g* centrifugation and subsequently washed for five times in 1 mL extraction buffer. After each wash step the beads were collected by 1,000*g* centrifugation. For SDS-PAGE, beads were boiled for 5 min in 60 μL, respectively, 15 μL, of 2× SDS loading buffer after the final wash step, and after centrifugation at 18,000*g* for 5 min the supernatant was loaded on gel.

Tryptic Digestion of Immunopurified Proteins

Immunopurified proteins were separated by 7% SDS-PAGE, after which the gel was stained with SimplyBlue Safestain Coomassie solution (Invitrogen) for 30 min and shortly destained using 10% ethanol/7.5% acetic acid (v/v) in water. For analysis on the Synapt MS (Waters), protein bands were excised from the gel and subjected to in-gel tryptic digestion. Gel slices were destained in 40% acetonitrile (ACN) in 0.1 M ammonium bicarbonate for 30 min and after air drying by vacuum centrifugation (Savant Speedvac), trypsin (10 ng/μL; sequence grade modified, Promega) was added (completely covering the gel slice), followed by overnight incubation at 37°C. Tryptic peptides were subsequently extracted with 50% ACN containing 0.1% trifluoroacetic acid (TFA; Fluka) and air dried by vacuum centrifugation.

In an alternative approach, GFP-trap_A beads used for the immunopurification were not boiled in SDS loading buffer to release the proteins, but the purified proteins were subjected to on-bead tryptic digestion. Hereto, beads were washed twice with 50 mM ammonium bicarbonate buffer (pH 8), after which the beads were incubated for 1 h at 60°C with 50 mM dithiothreitol in 50 mM ammonium bicarbonate. Subsequently, 50 mM iodoacetamide in 50 mM ammonium bicarbonate was added and beads were incubated at room temperature in the dark for another hour. Next, 50 mM Cys was added and directly thereafter 1 μL of trypsin (Roche) solution (0.5 μg, in 1 mM HCl) was added to the solution. Beads were incubated overnight at 20°C, after which the digestion was terminated by adding TFA to a final concentration of 0.5% (v/v). For analysis on the Orbitrap XL (Thermo Scientific), proteins were stored at −20°C until further analysis. For analysis on the Synapt MS (Waters), after centrifugation at 15,000*g* for 10 min, the peptides were cleaned by binding them to a SupelClean LC-18 1-mL SPE column (Supelco) equilibrated with 0.1% TFA. Peptides were then eluted with 60% ACN containing 0.1% formic acid (Merck), were dried down by vacuum centrifugation, and dissolved in 20 μL of 0.1 M ammonium formate (pH 10) prior to two-dimensional liquid chromatography-mass spectrometry analysis. For technical details on protein identification by mass spectrometry on the Synapt MS and Orbitrap XL and subsequent data processing we refer to the Supplemental Materials and Methods S1.

Phylogenetic Analysis of BiP and CRT Families

Phylogenetic analysis of BiP and CRT sequences was performed using the online Web service Phylogeny.fr at www.phylogeny.fr (Dereeper et al., 2008). We used MUSCLE for multiple sequence alignments and PhylML for tree building. TreeDyn was used for tree rendering.

Confocal Microscopy

Confocal microscopy was performed on *Agrobacterium*-infiltrated *N. benthamiana* leaves, employing a Carl Zeiss LSM 510 META confocal microscope equipped with a Plan-Apochromat 63×/1.4 oil differential interference contrast objective. eGFP and chlorophyll were excited using an argon laser beam at 488 nm and emission from eGFP and chlorophyll was detected using the 505 to 530 nm band-pass filter and the 650 long-band filter, respectively.

Immunoblotting and Silver Staining

Immunopurified proteins were separated by 8% SDS-PAGE and transferred to an Immun-Blot polyvinylidene difluoride membrane (Bio-Rad) using overnight electro blotting at 25 V. The membrane was incubated with blocking solution containing 5% skimmed milk powder and, to detect GFP fusion proteins, blots were incubated with 1:5,000 diluted αGFP-HRP (Anti-GFP-HRP, 130-091-833, MACS antibodies). For detection of BiP, blots were first incubated with 1:1,000 diluted αBiP (BiP-95, sc-33757, Santa Cruz) and subsequently with 1:2,000 diluted goat anti-rabbit-HRP (anti-rabbit IgG-HRP, A9169, Sigma). For detection of complex glycans, blots were first incubated with 1:2,000 diluted αHRP (rabbit anti-HRP, 323-005-021, Jackson ImmunoResearch) and then incubated with 1:2,000 diluted goat anti-rabbit-HRP. Detection of Myc was performed by 1:2,000 diluted cMyc (cMyc 9E10, sc-40, Santa Cruz) and subsequently 1:2,000 diluted anti-Mouse Ig-HRP (Amersham). In-gel silver staining was performed as described previously (Blum et al., 1987).

Generation of Constructs for VIGS

Fragments of genes to be used for VIGS were amplified by PCR on tomato or *N. benthamiana* cDNA. A VIGS fragment for Sl-*BiP1* was amplified using primers to137 and to138 and a VIGS fragment for Sl-*BiP2* was amplified using primers to139 and to140. VIGS fragment Sl-*BiP4* was amplified by primers to141 and to142. All VIGS fragments were cloned into pCR4-TOPO (Invitrogen) and the sequences were verified. The VIGS fragments were *Eco*RI excised from pCR4-TOPO and cloned into *Eco*RI-linearized pTRV-RNA2 (pYL156; Liu et al., 2002a, 2002b), to generate pTRV:Sl-*BiP1* (Sol 2730), pTRV:Sl-*BiP2* (Sol 2731), and pTRV:Sl-*BiP4* (Sol 2732).

VIGS fragment Sl-*BiP3* was amplified with primers to201 and to202 and a fragment targeting Sl-*BiP1*, Sl-*BiP2*, and Sl-*BiP4* (Sl-*BiP-1*, *-2*, and *-4*) was amplified using primer combination to176 and to177. A fragment for Sl-*CRT2* was amplified by primers to170 and to171 and a fragment for Sl-*CRT3b* was amplified with to174 and to175. Fragments Nb-*CRT3a* and Sl-*CRT3a* were amplified with primers pairs to213/to214 and to172/to173, respectively. Fragments Sl-*BiP3*, Sl-*BiP1*, *-2*, and *-4*, Sl-*CRT2*, Nb-*CRT3a*, Sl-*CRT3a*, and Sl-*CRT3b* were cloned into pCR4-TOPO and sequenced for the correct insert. Fragment Sl-*BiP1*, *-2*, and *-4* was excised from pCR4-TOPO using restriction enzymes *Xba*I and *Bam*HI and cloned into pTRV-RNA2, linearized with the same restriction enzymes, to generate pTRV:Sl-*BiP1*, *-2*, and *-4* (Sol 2771). Fragment Sl-*BiP3* was excised from pCR4-TOPO using restriction enzymes *Bam*HI and *Xho*I and cloned into pTRV-RNA2, linearized with the same restriction enzymes to generate pTRV:Sl-*BiP3* (Sol 2793). The Sl-*BiP3* fragment was cloned into Sol 2771, linearized with *Bam*HI and *Xho*I, to generate pTRV:Sl-*BiP1*, *-2*, *-3*, and *-4* (Sol 2792). PCR fragments Sl-*CRT2*, Nb-*CRT3a*, Sl-*CRT3a*, and Sl-*CRT3b* were excised from pCR4-TOPO by *Eco*RI and *Bam*HI and cloned in pTRV-RNA2 linearized with the same restriction enzymes to generate pTRV:Sl-*CRT2* (Sol 2768), pTRV:Nb-*CRT3a* (Sol 2803), pTRV:Sl-*CRT3a* (Sol 2769), and pTRV:Sl-*CRT3b* (Sol 2770).

VIGS in *N. benthamiana*, qRT-PCR, and HR Assays

Four-week-old wild-type (for qRT-PCRs) or transgenic *N. benthamiana*:*Cf-4* (for HR assay) plants were inoculated by *Agrobacterium*-mediated expression with pTRV-RNA1 and the pTRV-RNA2 constructs described above targeting

the different ER-QC genes (Liu et al., 2002a, 2002b). TRV:*Cf-4* (Gabriëls et al., 2006), TRV:PDS (Liu et al., 2002a, 2002b), and TRV:*GUS* (Tameling and Baulcombe, 2007) were mixed with pTRV-RNA1 and served as controls. For silencing of *SGT1* we infiltrated the pTV00-derived constructs pBINTRA6 (binary TRV-RNA1 vector) and TRV:*SGT1* (Ratcliff et al., 2001; Peart et al., 2002). All agroinoculations were done in a 1:1 ratio with a final OD_{600} = 0.8 for each construct and photographs were taken 3 weeks after inoculation with the recombinant virus.

For qRT-PCR, single leaves of recombinant TRV-inoculated wild-type *N. benthamiana* were harvested per VIGS treatment. Total RNA was extracted from ground leaf material using the NucleoSpin RNA plant kit (Macherey-Nagel). First-strand cDNA synthesis was performed using moloney-murine leukemia virus reverse transcriptase (Promega) and an oligo(dT) primer. qRT-PCR was done according to the protocol of the SensiMix SYBR kit (Bioline). Nb-*CRT2* expression was examined using primers to203 and to204, Nb-*CRT3a* expression with primers to205 and to206, and Nb-*CRT3b* expression with primers to207 and to208. Endogenous Nb-*Actin* was amplified using primers to58 and to59. qRT-PCR was performed on an ABI7300 machine (Applied Biosystems) using the following cycles; 95°C for 10 min, followed by 40 cycles of 95°C for 15 s and 60°C for 45 s, PCR products were not derived from genomic DNA contamination, as control samples omitting moloney-murine leukemia virus reverse transcriptase did not result in a PCR product after 40 amplification cycles (data not shown).

For the HR assay, 3 weeks after inoculation of *N. benthamiana*:*Cf-4* with the various VIGS constructs, mature leaves above the inoculated leaves were infiltrated with *A. tumefaciens* directing expression of Avr4 (pMOG800-Avr4, pRH87; Van der Hoorn et al., 2000) at OD_{600} = 0.03 (Gabriëls et al., 2007), RxD460V [pB1-Rx (AT39-H1; D460V); Bendahmane et al., 2002] at OD_{600} = 0.1, and BAX (Lacomme and Santa Cruz, 1999) at OD_{600} = 0.5. Three days after *Agrobacterium*-mediated expression of the elicitors, leaves were examined for the development of an HR.

VIGS in Tomato, *Cladosporium fulvum* Disease Assay, and Quantification of *C. fulvum* Growth

Cotyledons of 10-d-old MM-Cf-0 tomato plants transformed with the *Hcr9-4D* (*Cf-4*) gene (Thomas et al., 1997), resistant to Avr4-producing strains of *C. fulvum* were agroinoculated with the pTRV-RNA1 and the pTRV-RNA2 constructs described above (Liu et al., 2002a, 2002b). TRV:*Cf-4* (Gabriëls et al., 2006), TRV:*PDS* (Liu et al., 2002a, 2002b), TRV:*GUS* (Tameling and Baulcombe, 2007), and TRV:*GFP* (Burch-Smith et al., 2006) were mixed with pTRV-RNA1 and served as controls. In *C. fulvum* disease assays, nonagroinoculated Hcr9-4D plants, fully resistant to the fungus, were included and non-agroinoculated MM-Cf-0 plants were included as fully susceptible controls. Agroinoculations were done in a 1:1 pTRV:RNA1 and pTRV:RNA2 ratio, with a final OD_{600} = 1 for each construct. Four tomato plants per treatment were used in each experiment.

For *C. fulvum* disease assays, 3 weeks after inoculation with the recombinant TRV viruses, plants were inoculated with conidia of the fungus as described previously (Stulemeijer et al., 2007). We used *C. fulvum* race 5 (secreting Avr4)-*pGPD*:*GUS*, expressing the *GUS* gene under control of the constitutive *GPD* promoter. Two weeks after inoculation with *C. fulvum*, colonization of all inoculated leaflets was studied by an X-glucuronide (Biosynth AG) stain to detect GUS activity. Quantification of blue-stained spots indicating fungal growth was done using the ImageJ plug-in Phenotype Quant in the Clado GUS Quant mode using the default settings (Abd-El-Haliem, 2012). The plug in determines the total area of blue-stained spots (indicating fungal growth) and the total leaf surface area. Average fungal colonization was calculated for three independent experiments. In each individual experiment the relative fungal growth on nonagroinoculated Hcr9-4D plants was used as a calibrator and all other treatments were normalized to this treatment. Statistical analysis was performed by a one-way ANOVA, followed by a Tukey's post hoc test.

Supplemental Data

The following materials are available in the online version of this article.

Supplemental Figure S1. Cf-eGFP fusion proteins are functional.

Supplemental Figure S2. Sequence alignment of the tomato Sl-*BiP* and *N. benthamiana* Nb-*BiP* genes.

Supplemental Figure S3. Tomato and *N. benthamiana* contain four BiP homologs and two CRT3 homologs.

Supplemental Figure S4. Silencing of individual *BiPs* does not affect Cf-4 function, whereas silencing of multiple *BiPs* causes lethality in *N. benthamiana*.

Supplemental Figure S5. Sequence alignment of the tomato Sl-*CRT* and *N. benthamiana* Nb-*CRT* genes.

Supplemental Figure S6. Transiently expressed Sl-CRT-eGFP proteins localize to the ER network.

Supplemental Figure S7. VIGS of the different Nb-*CRTs* does not result in an aberrant phenotype in *N. benthamiana*.

Supplemental Table S1. Scores of peptides identified by mass spectrometry.

Supplemental Table S2. Sequences of all oligonucleotide primers used.

Supplemental Materials and Methods S1. Technical details of mass spectrometry analysis for protein identification and data processing.

ACKNOWLEDGMENTS

We thank Renier van der Hoorn for helpful discussions. We appreciate the suggestions from Sander van der Krol and Maurice Henquet for using the αHRP antibody. Chris Maliepaard is acknowledged for help with the statistics. We thank Daniela Sueldo for generating the GFP-HA construct. We appreciate the useful suggestions on the immunopurifications from Catherine Albrecht. Norbert de Ruijter is acknowledged for assistance with confocal microscopy. Bert Essenstam and Henk Smid are acknowledged for excellent plant care. T.W.H.L. and M.H.A.J.J. designed research and analyzed data with input from P.S., J.H.G.C., A.H.P.A., A.M.E.J., S.R., B.P.H.J.T., and W.I.L.T.; T.W.H.L., P.S., J.H.G.C., A.H.P.A., J.S., and A.M.E.J. performed experiments. A.A.E.H. and R.J. contributed new analytic tools. T.W.H.L. and M.H.A.J.J. wrote the manuscript with contributions from the other authors.

Received March 5, 2012; accepted May 24, 2012; published May 30, 2012.

LITERATURE CITED

Abd-El-Haliem AM (2012) An unbiased method for the quantitation of disease phenotypes using a custom-built macro plugin for the program ImageJ. Methods Mol Biol **835:** 635–644

Anelli T, Alessio M, Bachi A, Bergamelli L, Bertoli G, Camerini S, Mezghrani A, Ruffato E, Simmen T, Sitia R (2003) Thiol-mediated protein retention in the endoplasmic reticulum: the role of ERp44. EMBO J **22:** 5015–5022

Anelli T, Sitia R (2008) Protein quality control in the early secretory pathway. EMBO J **27:** 315–327

Bendahmane A, Farnham G, Moffett P, Baulcombe DC (2002) Constitutive gain-of-function mutants in a nucleotide binding site-leucine rich repeat protein encoded at the *Rx* locus of potato. Plant J **32:** 195–204

Blum H, Beier H, Gross HJ (1987) Improved silver staining of plant proteins, RNA and DNA in polyacrylamide gels. Electrophoresis **8:** 93–99

Boller T, Felix G (2009) A renaissance of elicitors: perception of microbe-associated molecular patterns and danger signals by pattern-recognition receptors. Annu Rev Plant Biol **60:** 379–406

Bolton MD, van Esse HP, Vossen JH, de Jonge R, Stergiopoulos I, Stulemeijer IJE, van den Berg GCM, Borrás-Hidalgo O, Dekker HL, de Koster CG, et al (2008) The novel Cladosporium fulvum lysin motif effector Ecp6 is a virulence factor with orthologues in other fungal species. Mol Microbiol **69:** 119–136

Burch-Smith TM, Schiff M, Liu Y, Dinesh-Kumar SP (2006) Efficient virus-induced gene silencing in Arabidopsis. Plant Physiol **142:** 21–27

Caplan JL, Zhu X, Mamillapalli P, Marathe R, Anandalakshmi R, Dinesh-Kumar SP (2009) Induced ER chaperones regulate a receptor-like kinase to mediate antiviral innate immune response in plants. Cell Host Microbe **6:** 457–469

Chisholm ST, Coaker G, Day B, Staskawicz BJ (2006) Host-microbe interactions: shaping the evolution of the plant immune response. Cell **124:** 803–814

Christensen A, Svensson K, Thelin L, Zhang W, Tintor N, Prins D, Funke N, Michalak M, Schulze-Lefert P, Saijo Y, et al (2010) Higher plant calreticulins have acquired specialized functions in Arabidopsis. PLoS ONE **5:** e11342

de Jong CF, Laxalt AM, Bargmann BOR, de Wit PJGM, Joosten MHAJ, Munnik T (2004) Phosphatidic acid accumulation is an early response in the *Cf-4/Avr4* interaction. Plant J **39:** 1–12

de Jonge R, van Esse HP, Kombrink A, Shinya T, Desaki Y, Bours R, van der Krol S, Shibuya N, Joosten MHAJ, Thomma BPHJ (2010) Conserved fungal LysM effector Ecp6 prevents chitin-triggered immunity in plants. Science **329:** 953–955

de Jonge R, van Esse HP, Maruthachalam K, Bolton MD, Santhanam P, Saber MK, Zhang Z, Usami T, Lievens B, Subbarao KV, et al (2012) Tomato immune receptor Ve1 recognizes effector of multiple fungal pathogens uncovered by genome and RNA sequencing. Proc Natl Acad Sci USA **109:** 5110–5115

Dereeper A, Guignon V, Blanc G, Audic S, Buffet S, Chevenet F, Dufayard JF, Guindon S, Lefort V, Lescot M, et al (2008) Phylogeny.fr: robust phylogenetic analysis for the non-specialist. Nucleic Acids Res (Web Server issue) **36:** W465–469

Gabriëls SHEJ, Takken FLW, Vossen JH, de Jong CF, Liu Q, Turk SCHJ, Wachowski LK, Peters J, Witsenboer HMA, de Wit PJGM, et al (2006) CDNA-AFLP combined with functional analysis reveals novel genes involved in the hypersensitive response. Mol Plant Microbe Interact **19:** 567–576

Gabriëls SHEJ, Vossen JH, Ekengren SK, van Ooijen G, Abd-El-Haliem AM, van den Berg GCM, Rainey DY, Martin GB, Takken FLW, de Wit PJ, et al (2007) An NB-LRR protein required for HR signalling mediated by both extra- and intracellular resistance proteins. Plant J **50:** 14–28

Gómez-Gómez L, Boller T (2000) FLS2: an LRR receptor-like kinase involved in the perception of the bacterial elicitor flagellin in *Arabidopsis*. Mol Cell **5:** 1003–1011

Gruber CW, Čemažar M, Heras B, Martin JL, Craik DJ (2006) Protein disulfide isomerase: the structure of oxidative folding. Trends Biochem Sci **31:** 455–464

Häweker H, Rips S, Koiwa H, Salomon S, Saijo Y, Chinchilla D, Robatzek S, von Schaewen A (2010) Pattern recognition receptors require *N*-glycosylation to mediate plant immunity. J Biol Chem **285:** 4629–4636

Henquet M, Lehle L, Schreuder M, Rouwendal G, Molthoff J, Helsper J, van der Krol S, Bosch D (2008) Identification of the gene encoding the α1,3-mannosyltransferase (ALG3) in *Arabidopsis* and characterization of downstream *n*-glycan processing. Plant Cell **20:** 1652–1664

Hong Z, Jin H, Tzfira T, Li J (2008) Multiple mechanism-mediated retention of a defective brassinosteroid receptor in the endoplasmic reticulum of *Arabidopsis*. Plant Cell **20:** 3418–3429

Jia XY, He LH, Jing RL, Li RZ (2009) Calreticulin: conserved protein and diverse functions in plants. Physiol Plant **136:** 127–138

Jin H, Hong Z, Su W, Li J (2009) A plant-specific calreticulin is a key retention factor for a defective brassinosteroid receptor in the endoplasmic reticulum. Proc Natl Acad Sci USA **106:** 13612–13617

Jin Y, Awad W, Petrova K, Hendershot LM (2008) Regulated release of ERdj3 from unfolded proteins by BiP. EMBO J **27:** 2873–2882

Jones JDG, Dangl JL (2006) The plant immune system. Nature **444:** 323–329

Kruijt M, Brandwagt BF, de Wit PJGM (2004) Rearrangements in the *Cf-9* disease resistance gene cluster of wild tomato have resulted in three genes that mediate Avr9 responsiveness. Genetics **168:** 1655–1663

Lacomme C, Santa Cruz S (1999) Bax-induced cell death in tobacco is similar to the hypersensitive response. Proc Natl Acad Sci USA **96:** 7956–7961

Laurent F, Labesse G, de Wit P (2000) Molecular cloning and partial characterization of a plant VAP33 homologue with a major sperm protein domain. Biochem Biophys Res Commun **270:** 286–292

Li J, Zhao-Hui C, Batoux M, Nekrasov V, Roux M, Chinchilla D, Zipfel C, Jones JDG (2009) Specific ER quality control components required for biogenesis of the plant innate immune receptor EFR. Proc Natl Acad Sci USA **106:** 15973–15978

Liu Y, Schiff M, Dinesh-Kumar SP (2002a) Virus-induced gene silencing in tomato. Plant J **31:** 777–786

Liu Y, Schiff M, Marathe R, Dinesh-Kumar SP (2002b) Tobacco *Rar1, EDS1* and *NPR1/NIM1* like genes are required for *N*-mediated resistance to tobacco mosaic virus. Plant J **30:** 415–429

Nakagawa T, Kurose T, Hino T, Tanaka K, Kawamukai M, Niwa Y, Toyooka K, Matsuoka K, Jinbo T, Kimura T (2007) Development of series of gateway binary vectors, pGWBs, for realizing efficient construction of fusion genes for plant transformation. J Biosci Bioeng **104:** 34–41

Nakatsukasa K, Brodsky JL (2008) The recognition and retrotranslocation of misfolded proteins from the endoplasmic reticulum. Traffic **9:** 861–870

Nekrasov V, Li J, Batoux M, Roux M, Chu ZH, Lacombe S, Rougon A, Bittel P, Kiss-Papp M, Chinchilla D, et al (2009) Control of the pattern-recognition receptor EFR by an ER protein complex in plant immunity. EMBO J **28:** 3428–3438

Nekrasov V, Ludwig AA, Jones JDG (2006) CITRX thioredoxin is a putative adaptor protein connecting Cf-9 and the ACIK1 protein kinase during the Cf-9/Avr9-induced defence response. FEBS Lett **580:** 4236–4241

Noh SJ, Kwon CS, Oh DH, Moon JS, Chung WI (2003) Expression of an evolutionarily distinct novel BiP gene during the unfolded protein response in *Arabidopsis thaliana*. Gene **311:** 81–91

Park CJ, Bart R, Chern M, Canlas PE, Bai W, Ronald PC (2010) Overexpression of the endoplasmic reticulum chaperone BiP3 regulates XA21-mediated innate immunity in rice. PLoS ONE **5:** e9262

Parniske M, Hammond-Kosack KE, Golstein C, Thomas CM, Jones DA, Harrison K, Wulff BBH, Jones JDG (1997) Novel disease resistance specificities result from sequence exchange between tandemly repeated genes at the *Cf-4/9* locus of tomato. Cell **91:** 821–832

Parniske M, Jones JDG (1999) Recombination between diverged clusters of the tomato *Cf-9* plant disease resistance gene family. Proc Natl Acad Sci USA **96:** 5850–5855

Pattison RJ, Amtmann A (2009) N-glycan production in the endoplasmic reticulum of plants. Trends Plant Sci **14:** 92–99

Peart JR, Lu R, Sadanandom A, Malcuit I, Moffett P, Brice DC, Schauser L, Jaggard DAW, Xiao S, Coleman MJ, et al (2002) Ubiquitin ligase-associated protein SGT1 is required for host and nonhost disease resistance in plants. Proc Natl Acad Sci USA **99:** 10865–10869

Persson S, Rosenquist M, Svensson K, Galvão R, Boss WF, Sommarin M (2003) Phylogenetic analyses and expression studies reveal two distinct groups of calreticulin isoforms in higher plants. Plant Physiol **133:** 1385–1396

Piedras P, Rivas S, Dröge S, Hillmer S, Jones JDG (2000) Functional, c-myc-tagged *Cf-9* resistance gene products are plasma-membrane localized and glycosylated. Plant J **21:** 529–536

Qiu Y, Xi J, Du L, Roje S, Poovaiah BW (2012) A dual regulatory role of *Arabidopsis* calreticulin-2 in plant innate immunity. Plant J **69:** 489–500

Ratcliff F, Martin-Hernandez AM, Baulcombe DC (2001) Technical advance: tobacco rattle virus as a vector for analysis of gene function by silencing. Plant J **25:** 237–245

Rivas S, Thomas CM (2005) Molecular interactions between tomato and the leaf mold pathogen *Cladosporium fulvum*. Annu Rev Phytopathol **43:** 395–436

Saijo Y, Tintor N, Lu X, Rauf P, Pajerowska-Mukhtar K, Häweker H, Dong X, Robatzek S, Schulze-Lefert P (2009) Receptor quality control in the endoplasmic reticulum for plant innate immunity. EMBO J **28:** 3439–3449

Schoberer J, Strasser R (2011) Sub-compartmental organization of Golgi-resident N-glycan processing enzymes in plants. Mol Plant **4:** 220–228

Schott A, Ravaud S, Keller S, Radzimanowski J, Viotti C, Hillmer S, Sinning I, Strahl S (2010) *Arabidopsis* stromal-derived Factor2 (SDF2) is a crucial target of the unfolded protein response in the endoplasmic reticulum. J Biol Chem **285:** 18113–18121

Stergiopoulos I, de Wit PJGM (2009) Fungal effector proteins. Annu Rev Phytopathol **47:** 233–263

Stulemeijer IJE, Stratmann JW, Joosten MHAJ (2007) Tomato mitogen-activated protein kinases LeMPK1, LeMPK2, and LeMPK3 are activated during the Cf-4/Avr4-induced hypersensitive response and have distinct phosphorylation specificities. Plant Physiol **144:** 1481–1494

Sun W, Cao Y, Jansen Labby K, Bittel P, Boller T, Bent AF (2012) Probing the *Arabidopsis* flagellin receptor: FLS2-FLS2 association and the contributions of specific domains to signaling function. Plant Cell **24:** 1096–1113

Tameling WIL, Baulcombe DC (2007) Physical association of the NB-LRR resistance protein Rx with a Ran GTPase-activating protein is required for extreme resistance to *Potato virus X*. Plant Cell **19:** 1682–1694

Thomas CM, Jones DA, Parniske M, Harrison K, Balint-Kurti PJ, Hatzixanthis K, Jones JDG (1997) Characterization of the tomato *Cf-4* gene for resistance to *Cladosporium fulvum* identifies sequences that determine recognitional specificity in Cf-4 and Cf-9. Plant Cell **9:** 2209–2224

van den Burg HA, de Wit PJGM, Vervoort J (2001) Efficient 13C/15N double labeling of the avirulence protein AVR4 in a methanol-utilizing strain (Mut+) of *Pichia pastoris*. J Biomol NMR **20:** 251–261

van den Burg HA, Harrison SJ, Joosten MHAJ, Vervoort J, de Wit PJGM (2006) *Cladosporium fulvum* Avr4 protects fungal cell walls against hydrolysis by plant chitinases accumulating during infection. Mol Plant Microbe Interact **19:** 1420–1430

Van der Hoorn RAL, Laurent F, Roth R, De Wit PJGM (2000) Agroinfiltration is a versatile tool that facilitates comparative analyses of *Avr9/Cf-9*-induced and *Avr4/Cf-4*-induced necrosis. Mol Plant Microbe Interact **13:** 439–446

van der Hoorn RAL, Wulff BBH, Rivas S, Durrant MC, van der Ploeg A, de Wit PJGM, Jones JDG (2005) Structure-function analysis of cf-9, a receptor-like protein with extracytoplasmic leucine-rich repeats. Plant Cell **17:** 1000–1015

van Esse HP, Bolton MD, Stergiopoulos I, de Wit PJGM, Thomma BPHJ (2007) The chitin-binding *Cladosporium fulvum* effector protein Avr4 is a virulence factor. Mol Plant Microbe Interact **20:** 1092–1101

Voinnet O, Rivas S, Mestre P, Baulcombe D (2003) An enhanced transient expression system in plants based on suppression of gene silencing by the p19 protein of tomato bushy stunt virus. Plant J **33:** 949–956

Wulff BBH, Kruijt M, Collins PL, Thomas CM, Ludwig AA, De Wit PJGM, Jones JDG (2004) Gene shuffling-generated and natural variants of the tomato resistance gene *Cf-9* exhibit different auto-necrosis-inducing activities in *Nicotiana* species. Plant J **40:** 942–956

Xu Q-F, Cheng W-S, Li S-S, Li W, Zhang Z-X, Xu Y-P, Zhou X-P, Cai X-Z (2012) Identification of genes required for Cf-dependent hypersensitive cell death by combined proteomic and RNA interfering analyses. J Exp Bot **63:** 2421–2435

Zipfel C, Kunze G, Chinchilla D, Caniard A, Jones JDG, Boller T, Felix G (2006) Perception of the bacterial PAMP EF-Tu by the receptor EFR restricts *Agrobacterium*-mediated transformation. Cell **125:** 749–760